Spontaneously Generated X-Shaped Light Bullets

P. Di Trapani,[1] G. Valiulis,[2] A. Piskarskas,[2] O. Jedrkiewicz,[1] J. Trull,[1] C. Conti,[3] and S. Trillo[3,4]

[1]*Istituto Nazionale di Fisica della Materia (INFM) and Department of Chemical, Physical and Mathematical Sciences, University of Insubria, Via Valleggio 11, 22100 Como, Italy*

[2]*Department of Quantum Electronics, Vilnius University, Sauletekio avenue 9, LT-2040 Vilnius, Lithuania*

[3]*Istituto Nazionale di Fisica della Materia (INFM)-RM3, Via della Vasca Navale 84, 00146 Roma, Italy*

[4]*Department of Engineering, University of Ferrara, Via Saragat 1, 44100 Ferrara, Italy*

(Received 17 March 2003; published 28 August 2003)

We observe the formation of an intense optical wave packet fully localized in all dimensions, i.e., both longitudinally (in time) and in the transverse plane, with an extension of a few tens of fsec and microns, respectively. Our measurements show that the self-trapped wave is an X-shaped light bullet spontaneously generated from a standard laser wave packet via the nonlinear material response (i.e., second-harmonic generation), which extend the soliton concept to a new realm, where the main hump coexists with conical tails which reflect the symmetry of linear dispersion relationship.

DOI: 10.1103/PhysRevLett.91.093904 PACS numbers: 42.65.Tg, 05.45.Yv, 42.65.Jx

Defeating the natural spreading of a wave packet (WP) is a universal and challenging task in any physical context involving wave propagation. Ideal particlelike behavior of WPs is demanded in applications such as microscopy, tomography, laser-induced particle acceleration, ultrasound medical diagnostics, Bose-Einstein condensation, volume optical-data storage, optical interconnects, and those encompassing long-distance or high-resolution signal transmission. The quest for light WPs that are both invariant (upon propagation) and sufficiently localized in all dimensions (3D, i.e., both transversally and longitudinally or in time) against spreading "forces" exerted by diffraction and material group-velocity dispersion (GVD, $k'' = d^2k/d\omega^2|_{\omega_0}$) has motivated long-standing studies, which have followed different strategies in the *linear* [1–5] and *nonlinear* [6,7] regimes, respectively.

In the linear case, to counteract material (intrinsic) GVD, one can exploit the angular dispersion (i.e., dependence of propagation angle on frequency) that stems from a proper WP shape. The prototype of such WPs is the X wave [2], a nonmonochromatic, yet nondispersive, superposition of nondiffracting cylindrically symmetric Bessel J_0 (so-called conical or Durnin [1]) beams, experimentally tested in acoustics [3], optics [4], and microwave antennas [5]. Importantly, in the relevant case of WPs with relatively narrow spectral content both temporally (around carrier frequency ω_0) and spatially (around propagation direction z, i.e., paraxial WPs), X waves require *normally* dispersive media ($k'' > 0$). In this case, a WP with disturbance $E(r, t, z)\exp(ik_0 z - i\omega_0 T)$ [$k_0 \equiv k(\omega_0)$, $r^2 \equiv x^2 + y^2$], has a slowly varying envelope $E = E(r, t, z)$ obeying the standard wave equation

$$\hat{L}(\omega_0)E = 0; \qquad \hat{L}(\omega_0) \equiv i\partial_z + \frac{1}{2k_0}\nabla_\perp^2 - \frac{k''}{2}\partial_{tt}^2, \quad (1)$$

Laplacian, where $\nabla_\perp^2 = \partial_{rr}^2 + r^{-1}\partial_r$ is the transverse Laplacian, and we limit our attention to luminal WPs traveling at light group velocity $1/k' = dk/d\omega|_{\omega_0}^{-1}$ by introducing the retarded time $t = T - k'z$ in the WP barycenter frame. Propagation-invariant waves $E(r, t, z) = E(r, t, z = 0)\exp(i\beta z)$ can be achieved whenever their input spatiotemporal spectra $E(K, \Omega, z = 0)$ lie along the characteristics of the dispersion relationship $k''\Omega^2/2 - K^2/(2k_0) = \beta$, which follows from Eq. (1) in Fourier space (K, Ω) (K is the transverse wave vector related to cone angle with z axis $\theta \simeq \sin\theta = K/k_0$, and $\Omega = \omega - \omega_0$). In the normal GVD regime ($k'' > 0$) these curves, displayed in Fig. 1(a), reflect the hyperbolic nature of the wave equation (1) and show the common

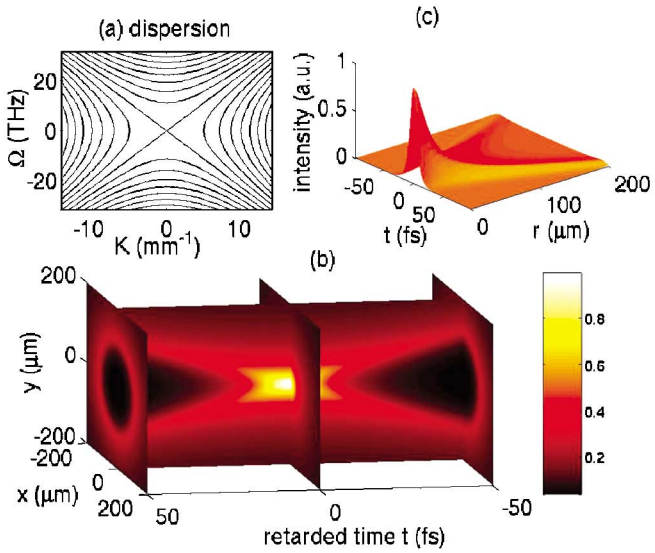

FIG. 1 (color). Features of normally dispersive media ($k'' > 0$). (a) spatiotemporal dispersion relation associated with paraxial wave Eq. (1). Different representations [(b) sections of color isointensity surfaces $|E(x, y, t)|^2 = \text{const}$; (c) intensity versus r, t] of a nondiffractive, nondispersive linear X wave ($\Delta = 10$ fs, $k'' = 0.02$ ps^2/m, $k_0 = 10^7$ m^{-1}).

asymptotic spectral X shape associated with the lines $K = \pm 2k_0 k'' \Omega$ ($\beta = 0$). When the spectral components lying along such X are superimposed coherently (in phase), the field in the physical space (r, t) also retains a propagation-invariant X shape, as entailed, e.g., by the exact solution $E = \mathrm{Re}\{[(\Delta - it)^2 + k_0 k'' r^2]^{-1/2}\}$ of Eq. (1) shown in Figs. 1(b) and 1(c). Here Δ represents duration of the X-wave central hump. Main features of these waves are the conical (clepsydra) 3D structure and the slow spatial decay ($1/r$ characteristic of J_0 components [1]), displayed in Figs. 1(b) and 1(c), respectively.

Conversely, in the nonlinear (high intensity) regime, nonspreading WPs exploit the idea that, in self-focusing media, the nonlinear wave front curvature can simultaneously balance the curvature due to diffraction and GVD, combining features of spatial [8] and temporal [9] solitons to form a bell-shaped 3D-localized WP $E(r, t)$, so-called light bullet [6]. In sharp contrast with X waves, such compensation strictly requires *anomalous* GVD ($k'' < 0$) [6], thus implying that along the WP tails, where Eq. (1) still holds true, space r and time t play the same role giving rise to strong WP localization [10]. Stable trapping, however, has been observed only in setting of reduced dimensionality (2D) [7,11], including also other contexts, e.g., spin [12] or atomic waves [13] (3D kinetic energy and atom-atom attractive interactions act exactly as diffraction GVD and self-focusing, respectively) where similar trapping mechanisms hold true.

In this work, we outclass the two approaches by demonstrating that *space-time localization in the normal GVD regime becomes accessible in the nonlinear regime.* Trapping is accomplished by mutual balance of intrinsic, shape-induced, and nonlinear contributions in a new type of WP, namely, a nonlinear X wave, which permits one to get over two limitations at once. First, in contrast with linear X waves, whose observation requires nontrivial input beam shaping [3,4], our experiment reveals a remarkable "mode-finding" process that, starting from a conventional (Gaussian) laser WP, spontaneously performs the reshaping into a localized X-shaped WP. Second, we believe this to be the first genuine nonlinear trapping in full-dimensional 3D physical space, since to date material and/or instability limitations [6,7] have rendered the observation of light 3D bullets elusive.

Figure 2 describes the strong localization features observed after propagation in a 22 mm long sample of lithium triborate (LBO) $\chi^{(2)}$ crystal. At the input we launch a laser WP at fundamental frequency (FF) $\omega_0 = 2\pi c/\lambda_0$, $\lambda_0 = 1060$ nm, with Gaussian profile in both t (with FWHM duration in the 100–200 fs range) and r (45 μm FWHM at waist, located a few mm before the crystal so that the input beam is slightly diverging). The LBO crystal is tuned for generation of optical second-harmonic (SH) in the regime of relatively large positive phase mismatch $\Delta k = 2k(\omega_0) - k(2\omega_0) = 30\ \mathrm{cm}^{-1}$ or effective self-focusing for the FF beam [14]. When the input energy exceeds about 0.25 μJ, mutually trapped

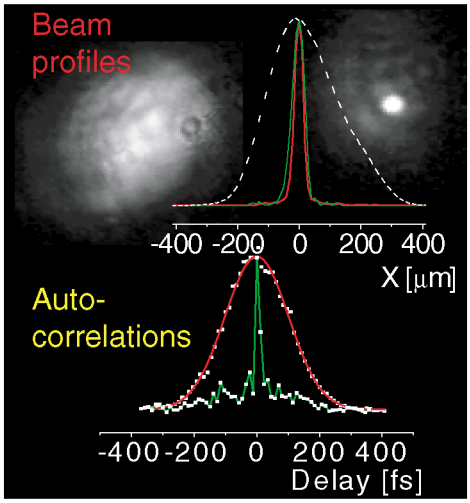

FIG. 2 (color). Top: output transverse beam profiles in the linear (white) and nonlinear (green: SH; red: FF) regime. The diffracted (left) and localized (right) spots recorded at the output of the crystal are also shown. Bottom: temporal autocorrelation traces (collinear technique) showing the transition from the linear regime (red) to the compressed WP (green).

localized WPs at FF and SH are observed (see Fig. 2). Time-integrated measurements of spatial profiles (Fig. 2, top) indicate that diffraction is fully defeated to yield a spatial solitonlike beam [8], while temporal autocorrelations reveal a single pulse which is strongly compressed (down to $\sim$20 fs; see Fig. 2, bottom). Remarkably, nonlinear mixing balances the two highest-order dispersive effects, namely, the tendency of FF and SH to walkoff due to group-velocity mismatch (GVM) $\delta V = k'(2\omega_0) - k'(\omega_0)$ and GVD, which act in the linear regime over characteristic length scales 50 and 2.5 times shorter than the crystal length, respectively. Relying on nonlinear scenarios known to date, the present result is unexpected. In fact, the normal GVD and the strong GVM of LBO do not allow an explanation in terms of light bullets, whereas the dynamics of self-focusing with normal GVD is dominated by pulse splitting without envisaging localization whatsoever [15].

In order to get a deeper understanding, we performed a set of numerical experiments by integrating the well-known model [14], which generalizes Eq. (1) to nonlinear coupling of envelopes $E_m(r, t, z)$ ($m = 1, 2$, carrier $m\omega_0$),

$$\begin{aligned} \hat{L}(\omega_0)E_1 + \chi E_2 E_1^* \exp(-i\Delta k z) &= 0, \\ \hat{L}(2\omega_0)E_2 + \delta V \partial_t E_2 + \chi E_1^2 \exp(i\Delta k z) &= 0. \end{aligned} \tag{2}$$

In Fig. 3 (top) we show snapshots of the space-time evolution. It is clear that, in the first stage ($z = 10$–15 mm), the generation of light at SH is accompanied by strong self-focusing, in turn inducing pulse compression (in spite of the normal GVD that would cause temporal broadening of plane waves). The WP becomes asymmetric since self-focusing is stronger where the SH,

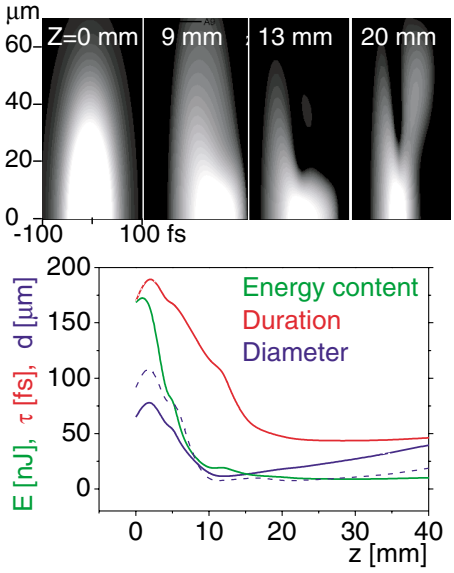

FIG. 3 (color). Numerical simulation of the localization process observed in our LBO sample [from Eqs. (2) with $k''(\omega_0) = 0.016\ \mathrm{ps}^2/\mathrm{m}$, $k''(2\omega_0) = 0.089\ \mathrm{ps}^2/\mathrm{m}$, $\delta V = 45\ \mathrm{ps/m}$, $\chi = 7 \times 10^{-5}\ \mathrm{W}^{-1/2}$ ($d_{\mathrm{eff}} = 0.85\ \mathrm{pm/V}$)] from an input Gaussian WP with 45 μm waist, 170 fs duration, and 0.26 μJ energy. Top: snapshots showing the FF beam in the t-x plane. Bottom: evolution of the beam diameter, duration, and energy content of main localized hump. The dashed line refers to more energetic (e.g., slightly wider and longer) input WPs for which even the small residual diffraction (solid line) is removed. In this case, however, the reshaping leads to higher peak intensity close to damage threshold of LBO.

which lags behind because of GVM, tends to be. More importantly, during this process the WP undergoes a strong reshaping, where a large fraction of energy is radiated off axis to form the tails of a conical wave (see snapshot at $z = 20$ mm). After this stage, however, the collapse stops and the WP propagates (locked with the SH) with immutable shape and nearly constant energy, duration, and size.

By changing the parameters in Eqs. (2) we can conclude that (i) nonlinearity is the key element that drives the reshaping and holds the WP together. In fact, by switching it off after the transient (i.e., $\chi = 0$ for $z > 20$ mm), the WP exhibits strong diffraction and extremely fast FF-SH walkoff. The reshaped WP can by no means be considered a linear X wave. (ii) In our crystal, GVM is the dominant dispersion term affecting the asymptotic duration and width of the localized WP (both decrease for smaller GVM). However, (symmetric) X-shaped WPs are formed also in the ideal case of vanishing GVM, provided that GVD is normal. (iii) The WP reshaping strongly affects the phase modulation process, which reveals the contribution of an effective anomalous GVD. (iv) By including additional cubic nonlinearities [14], the phenomenon remains qualitatively unchanged.

A more rigorous ground for explaining the dramatic reshaping shown in Fig. 3 is offered by the linear stability analysis of z-invariant solutions of Eqs. (2) with ideally vanishing spatiotemporal spectral width (i.e., continuous plane waves), which reveals the presence of exponentially growing weak (up to noise level) perturbations with definite frequency K, Ω. In fact, the instability features reflect the symmetry of the linear wave equation, thus being qualitatively different in the normal and anomalous GVD regime, respectively. While anomalous GVD leads to narrow bandwidth features as in conventional spatial or temporal modulational instability [14], the hyperbolic structure of the diffraction-dispersion operator in the normal GVD regime of our experiment leads to exponential amplification of conical wave perturbations (Bessel J_0 beams) with frequencies basically approaching the asymptotes of Fig. 1(a) [16]. When growing spontaneously from noise, the amplified components in the virtual infinite bandwidth [in reality limited by nonparaxiality and higher-order dispersion not accounted for in Eqs. (1) and (2)] leads to colored conical emission. Our calculations show that the phenomenon persists under dynamical conditions (unseeded SH generation) and when pumped by short-pulse narrow-beam inputs, as in our experiment. In the latter case, the amplification of proper frequency components of the WP preserves the mutual phase coherence, thus acting as a trigger which drives the transformation of the WP into the X wave shown in Fig. 3. In other words, it is the conical instability that probes the symmetry of the underlying linear system in amplifying those components which allow both diffraction and dispersion of the whole WP to be removed.

A second, strong argument in favor of the nearly asymptotic character of the evolution shown in Fig. 3 is the existence of stationary localized solutions of Eqs. (2). We have recently shown, indeed, that the natural propagation-invariant [i.e., with dependence $E_m(r, t) \times \exp(im\beta z)$, $m = 1, 2$] localized eigensolutions of SH generation process in the normal GVD regime (either with or without GVM) are indeed nonlinear X waves [17]. These waves are similar to those shown in Figs. 1(b) and 1(c) except for the fact that their peak intensity is related to their duration and width through the nonlinearity.

Since the measurements in Fig. 2 give information only about the WP central hump, in order to confirm experimentally that the observed strong focusing and compression dynamics is indeed driven by the formation of an X wave, we have performed different additional measurements. First, we have characterized the propagation of the WP in air after the LBO nonlinear crystal. We observe that the beam diffracts less than a Gaussian beam of the same width (the divergence angle is 2.5 times less), and this net sub-Gaussian diffraction witnesses a Bessel-like feature of the WP. Moreover, temporal broadening to 150 fs after only 10 cm of propagation in air is an indication that the WP develops strong angular dispersion (see Ref. [18] for the details). Both observations are in good quantitative agreement with data obtained numerically from Eqs. (2). However, it is only the tomography of

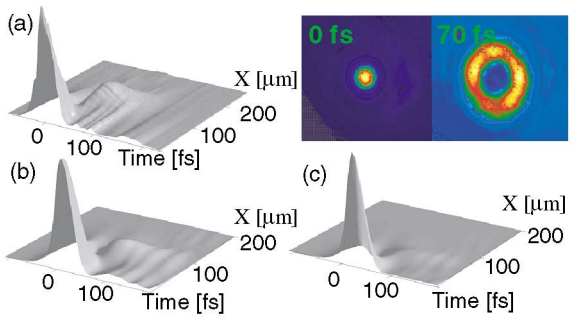

FIG. 4 (color). (a) Output spatiotemporal intensity profile, as measured in air, 5 mm from the crystal output face. Insets: transverse intensity pattern in (x, y) plane measured at peak ($t = 0$ fs) and with $t = 70$ fs delay. (b) As in (a), numerical result from Eqs. (2). (c) As in (b), calculated right on crystal output.

the output WP, i.e., mapping the WP intensity in space and time, that can give direct unequivocal evidence for the formation of an X wave. To this end we have developed a new technique based on an ultrafast nonlinear gating, or a scanning cross-correlation technique, realized by frequency mixing the WP under investigation with a 20 fs, high contrast, steep front, probe pulse in the visible, in a very thin (20 μm) BBO crystal [19]. The intensity map of the output WP is reported in Fig. 4(a). The measured profile clearly shows the features of an X wave with a conical structure, which emanates from a strongly localized central spatiotemporal hump. Unlike conventional pulse splitting [15], here splitting occurs only sufficiently off axis ($x \sim 100$ μm) in the WP low-intensity portion. For comparison we also report in Fig. 4(b) the profile calculated from Eqs. (2) under the same conditions, the agreement being excellent. The fringelike structure that appears for large delays in both Figs. 4(a) and 4(b) is due to 5 mm of free-space propagation in air outside the crystal. Although the calculated profile on the output face of the crystal indeed shows that such fringes disappear [see Fig. 4(c)], measurement with perfect imaging on the output LBO face reveals saturation of the mixing process due to a too intense peak.

In summary, we have reported the first evidence that the natural 3D (temporal and spatial) spreading of a focused ultrashort wave packet can be balanced in transparent materials at high intensity. The underlying mechanism is the *spontaneous* formation of an X wave characterized by an intense (i.e., nonlinear) central hump self-trapped through mutual balance with (essentially linear) dispersive contributions associated with coexisting slowly decaying conical tails. While our experiment is carried out by exploiting self-focusing nonlinearities arising from quadratic nonlinearity, we envisage the general role that self-trapping mediated by nonlinear X waves can have for a wide class of materials and applications encompassing centrosymmetric optical (Kerr) media [6], Bose-Einstein condensation [13], and acoustics [3].

We acknowledge support from MIUR (PRIN-01 and FIRB-01 projects), Unesco UVO-ROSTE (Contract No. 875.586.2), Secretaria de Estado y Universidades in Spain, and Fondazione Tronchetti Provera in Italy.

[1] J. Durnin, J. J. Miceli, and J. H. Eberly, Phys. Rev. Lett. **58**, 1499 (1987).
[2] E. Recami, Physica (Amsterdam) **252A**, 586 (1998); J. Salo, J. Fagerholm, A. T. Friberg, and M. M. Salomaa, Phys. Rev. Lett. **83**, 1171 (1999); Phys. Rev. E **62**, 4261 (2000).
[3] J. Lu and J. F. Greenleaf, IEEE Trans. Ultrason. Ferroelectr. Freq. Control **39**, 441 (1992).
[4] P. Saari and K. Reivelt, Phys. Rev. Lett. **79**, 4135 (1997); H. Snajalg, M. Rtsep, and P. Saari, Opt. Lett. **22**, 310 (1997).
[5] D. Mugnai, A. Ranfagni, and R. Ruggeri, Phys. Rev. Lett. **84**, 4830 (2000).
[6] Y. Silberberg, Opt. Lett. **15**, 1282 (1990); F. Wise and P. Di Trapani, Opt. Photonics News **13**, No. 2, 28 (2002), and references therein.
[7] X. Liu, L. J. Quian, and F. W. Wise, Phys. Rev. Lett. **82**, 4631 (1999); X. Liu, K. Beckwitt, and F. W. Wise, Phys. Rev. Lett. **85**, 1871 (2000).
[8] *Spatial Solitons*, edited by S. Trillo and W. E. Torruellas (Springer, Berlin, 2001).
[9] L. F. Mollenauer, R. H. Stolen, and J. P. Gordon, Phys. Rev. Lett. **45**, 1095 (1980).
[10] Mathematically the strong localization is associated with existing solutions $E(r, t)\exp(i\beta z)$ of Eq. (1) with $k'' < 0$, $\beta > 0$, which decay exponentially in $r, t \to \infty$.
[11] H. S. Eisenberg, R. Morandotti, Y. Silberberg, S. Bar-Ad, D. Ross, and J. S. Aitchison, Phys. Rev. Lett. **87**, 043902 (2001).
[12] M. Bauer, O. Buttner, S. O. Demokritov, B. Hillebrands, V. Grimalsky, Y. Rapoport, and A. N. Slavin, Phys. Rev. Lett. **81**, 3769 (1998).
[13] L. Khaykovich, F. Schreck, G. Ferrari, T. Bourdel, J. Cubizolles, L. D. Carr, Y. Castin, and C. Salomon, Science **296**, 1290 (2002); K. E. Strecker, G. B. Partridge, A. G. Truscott, and R. G. Hulet, Nature (London) **417**, 150 (2002).
[14] A. V. Buryak, P. Di Trapani, D. Skryabin, and S. Trillo, Phys. Rep. **370**, 63 (2002).
[15] J. K. Ranka, R. W. Schirmer, and A. L. Gaeta, Phys. Rev. Lett. **77**, 3783 (1996).
[16] S. Trillo, C. Conti, P. Di Trapani, O. Jedrkiewicz, J. Trull, G. Valiulis, and G. Bellanca, Opt. Lett. **27**, 1451 (2002).
[17] C. Conti, S. Trillo, P. Di Trapani, G. Valiulis, A. Piskarskas, O. Jedrkiewicz, and J. Trull, Phys. Rev. Lett. **90**, 170406 (2003).
[18] O. Jedrkiewicz, J. Trull, G. Valiulis, A. Piskarskas, C. Conti, S. Trillo, and P. Di Trapani, Phys. Rev. E (to be published).
[19] J. Trull, A. Matijosius, A. Varanavicius, O. Jedrkiewicz, G. Valiulis, R. Danielius, E. Kucinskas, A. Piskarskas, S. Trillo, and P. Di Trapani (to be published).